View metadata, citation and similar papers at core.ac.uk

brought to you by CORE

provided by Missouri University of Science and Technology (Missouri S&T): Scholars' Mine

Missouri University of Science and Technology

Scholars' Mine

International Specialty Conference on Cold-Formed Steel Structures

(2014) - 22nd International Specialty Conference on Cold-Formed Steel Structures

Nov 5th, 12:00 AM - 12:00 AM

Shape Optimisation of Cold-Formed Steel Profiles with Manufacturing Constraints - Part I: Algorithm

Bin Wang

Benoit P. Gilbert

Adrien M. Molinier

Hong Guan

Lip H. Teh

Follow this and additional works at: https://scholarsmine.mst.edu/isccss

 Part of the Structural Engineering Commons

Recommended Citation

Wang, Bin; Gilbert, Benoit P.; Molinier, Adrien M.; Guan, Hong; and Teh, Lip H., "Shape Optimisation of Cold-Formed Steel Profiles with Manufacturing Constraints - Part I: Algorithm" (2014). *International Specialty Conference on Cold-Formed Steel Structures*. 2.
https://scholarsmine.mst.edu/isccss/22iccfss/session01/2

This Article - Conference proceedings is brought to you for free and open access by Scholars' Mine. It has been accepted for inclusion in International Specialty Conference on Cold-Formed Steel Structures by an authorized administrator of Scholars' Mine. This work is protected by U. S. Copyright Law. Unauthorized use including reproduction for redistribution requires the permission of the copyright holder. For more information, please contact scholarsmine@mst.edu.

Twenty-Second International Specialty Conference on Cold-Formed Steel Structures
St. Louis, Missouri, USA, November 5 & 6, 2014

Shape optimisation of cold-formed steel profiles with manufacturing constraints - Part I: Algorithm

Bin Wang[1], Benoit P. Gilbert[2], Adrien M. Molinier[3], Hong Guan[4], Lip H. Teh[5]

Abstract

This paper presents a Genetic Algorithm optimisation method with manufacturing constraints for shape optimisation of cold-formed steel (CFS) profiles. Previous studies on unconstrained shape optimisation of CFS cross-sections, where the sole aim was to optimise the weight-to-capacity ratio of the profiles, yielded cross-sections that cannot be manufactured. Current cold-forming processes, such as roll-forming and brake-pressing, have limited ability to form continuously curved surfaces without discrete bends. This paper defines simple manufacturing rules and introduces them into the evolutionary algorithm. Augmented Lagrangian constraint-handling technique, with equality and inequality constrained violations, is used to avoid ill-conditioned problems. The ability and accuracy of the algorithm to handle the defined manufacturing constraints are verified by implementing it to optimise the section capacity of bisymmetric closed thin-walled profiles, for which an analytical solution is known.

[1] PhD Candidate, Griffith School of Engineering, Griffith University, Australia (b.wang@griffith.edu.au)
[2] Senior Lecturer, Griffith School of Engineering, Griffith University, Australia (b.gilbert@griffith.edu.au)
[3] Exchange undergraduate student, Griffith School of Engineering, Griffith University, Australia
[4] Associate Professor, Griffith School of Engineering, Griffith University, Australia (h.guan@griffith.edu.au)
[5] Senior Lecturer, School of Civil, Mining and Environmental Engineering, University of Wollongong, Australia (lteh@uow.edu.au)

1. Introduction

Compared to more "conventional" building materials, such as hot-rolled steel, concrete and timber, cold-formed steel (CFS) profiles possess a high capacity-to-weight ratio (Hancock, 2007). This feature makes CFS an attractive and cost-effective building solution.

CFS members are typically formed by bending coils of thin steel sheets (up to 0.236 inch (6 mm) thick) with a number of rollers (roll-forming) or die blocks (brake-pressing), as described later in Section 3.1. The manufacturing process allows the cross-sections to be shaped into almost any desired shape, tailoring the profiles to specific applications. However, despite this flexibility, the use of CFS sections has been mainly restricted to conventional C, Z or Σ cross-sectional shapes, with and without local stiffeners, as shown in Fig. 1. Taking full advantage of the nature of CFS structures by finding new optimised cross-sectional shapes for specific applications will enhance the competitiveness of CFS structures. Recent structural design methods such as the Direct Strength Method (DSM) (Schafer, 2008) have opened paths to innovation and facilitate the design of complex cross-sectional shapes.

Fig. 1. Conventional CFS profiles with or without stiffeners

For shape discovery, i.e. the ability to optimise the cross-sectional shape of a profile without presumption of its final shape, Simulated Annealing (SA) algorithm (Leng et. al., 2011) and Genetic Algorithm (GA) (Gilbert et. al., 2012a), combined with constraint-handling methods, represent useful tools to optimise cross-sectional shapes with no or limited influence from either human errors, arbitrary decisions or domain knowledge (Griffiths and Miles, 2003).

This paper aims at defining simple roll-forming (or brake-pressing) manufacturing rules. The existing "self-shape optimisation" algorithm (Gilbert et. al., 2012a, b) is improved by introducing the simple manufacturing rules into the algorithm. The algorithm is verified against a well-known optimisation problem, i.e. the shape optimisation of a doubly-symmetric (bisymmetric) closed CFS section for given second moments of area. The algorithm is subsequently used in the companion paper (Wang et. al., 2014) to optimise CFS manufacturable columns.

2. Literature review

2.1. General

In the last decade, shape optimisation of CFS sections ((Liu et. al., 2004), (Leng et. al., 2011), (Gilbert et. al., 2012a, b) and (Moharrami et. al., 2014)) has attracted increasing interests to extend dimension optimisation of known cross-sectional shapes ((Lee et. al., 2005) and (Lu and Mäkeläinen, 2006) for instance).

One of the early study on shape optimisation of CFS profiles is attributed to Liu et. al. (2004). A knowledge-based global optimisation algorithm, aiming at optimising the capacity of CFS columns manufactured from coils of set width and thickness, was used. Leng et. al. (2011) optimised the cross-sectional shapes of CFS open columns using three different optimisation algorithms, namely gradient-based steepest descent method, GA and Simulated Annealing (SA). Sections having a wall thickness of 1 mm and a perimeter of 280 mm were divided into 21 elements and optimised. ‘‘Open circular’’ and ‘‘S’’ cross-sections were found. Moharrami et. al. (2014) improved the study of Leng et. al. (2011) by introducing various types of boundary conditions into the algorithm. Gilbert et. al. (2012a, b) proposed a GA-based Augmented Lagrangian (AL) constraint-handling shape optimisation method for CFS profiles. The accuracy of the algorithm was verified against an optimisation problem for which an analytical solution is known. The cross-sectional shape of CFS open-section and simply supported columns, subjected to a set axial compression load, was optimised. A specific set of rules to accurately determine the local and distortional compressive elastic buckling stresses from Finite Strip signature curves was also developed. Despite of such research efforts made in the past, manufacturing constraints were not considered in these studies.

Manufacturing constraints were first introduced into shape optimisation algorithms for CFS profiles by Leng et. al. (2012) and Franco et. al. (2014). Leng et. al. (2012) introduced construction and partial manufacturing constraints into the shape optimisation of CFS columns using SA algorithm. The constraints were implemented for a CFS section by defining (i) flat “horizontal” flanges (ii) minimum dimensions for the “vertical” web, flanges and lips and (iii) allowance passage for utilities between lips. The web and lips were not optimised to be flat segments. The study was further improved in Leng et. al. (2013) by introducing a limited number of rollers (representing the number of discrete bends between flat segments). This resulted in manufacturable and improved section capacities, when compared to conventional Cee-sections of identical cross-sectional area.

Franco et. al. (2014) proposed promising CFS shape grammar rules, with an "alphabet", for shape optimisation of CFS profiles. Manufacturing constraints, with given stiffener sizes, are intrinsic to the shape grammar resulting in manufacturable cross-sections. GA is used by Franco et. al. (2014) as a search algorithm.

2.2. Self-shape optimisation and GA

The algorithm referred to as "self-shape optimisation" and developed by the senior authors (Gilbert et. al., 2012a, b) is used in the current study. The method consists of rigorously exploring the natural evolution process and the latent potential of Genetic Algorithm in an innovative way. GA was initially developed by Holland (1975) and is an adaptive heuristic search algorithm that mimics the Darwin's evolutionary survival of the fittest theory. It is less susceptible to be self-trapped into local optima and able to handle non-linear problems. The classical GA principles can be found in Adeli and Sarma (2006).

GA is an unconstrained optimisation method, and constrained problems are transformed into unconstrained problems by the use of a fitness function f expressed as

$$f = f(x) + \sum_{i=1}^{n} \alpha_i g_i(x) + \sum_{i=n+1}^{k} \beta_i h_i(x) \tag{1}$$

where $f(x)$ is the objective function, x is the vector of design variables, $g_i(x)$ and $h_i(x)$ are the i^{th} inequality and equality constraint violations (n inequality and k-n equality constraints), respectively, α_i and β_i are penalty factors. The algorithm aims to either maximise or minimise f.

In this research, the Augmented Lagrangian constraint-handling method for GA proposed by Adeli and Cheng (1994) is used. The fitness function f is then re-arranged as

$$f = f(x) + \frac{1}{2}\left\{ \sum_{i=1}^{n} \gamma_i \left\{ \left[g_i(x) + \mu_i \right] \right\}^2 + \sum_{i=n+1}^{k} \gamma_i \left[h_i(x) + \mu_i \right]^2 \right\} \tag{2}$$

where γ_i and μ_i are penalty function coefficients and real parameters associated with the i^{th} inequality and equality constraint, respectively. γ_i and μ_i are updated at each GA generation, see Adeli and Cheng (1994) for more details.

The main characteristics of the self-shape optimisation principle (Gilbert et. al., 2012a) are summarised as:

- The initial population in GA is generated by arbitrarily drawing cross-sections using self-avoiding random walks in a defined design space. Such random walks enable generating cross-sections without presumptions of their shapes.
- A floating-point type GA is used, meaning a cross-section is not defined using typical binary strings, but by floating-point numbers representing the coordinates of the points constituting the cross-section.
- Cross-over and mutation operators are performed in relation to the design space and not to the floating-point variables as in traditional GA. This operator allows for the merging of two cross-sections to generate off-springs bearing similarity in cross-sectional shapes to the two parents. In the mutation operator, a part of the cross-section is deleted and redrawn.

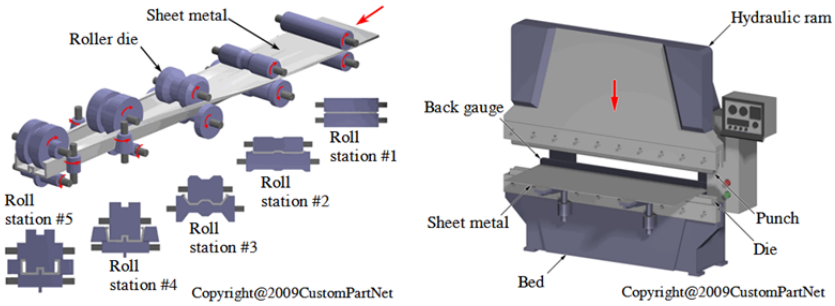

(a) (b)

Fig. 2. Cold-forming processes (a) roll-forming and (b) brake-pressing (Courtesy of CustomPartNet Inc.)

3. Manufacturing constraints

3.1. Traditional manufacturing processes

CFS profiles are typically mass-produced by two main cold-forming processes, referred to as “roll-forming” or “brake-pressing”. Both processes consist of bending a flat sheet of metal to the desired cross-sectional shape. In roll-forming operations, as shown in Fig. 2(a), the sheet is gradually rolled to the desired cross-sectional shape through successive rollers. This continuous manufacturing process allows long profiles to be manufactured. In brake-pressing operations, as shown in Fig. 2(b), the sheet is repetitively pressed between differently shaped

brake punches and die blocks to bend the desired cross-sectional shape. Brake-pressing is limited in manufacturing long members. Both manufacturing processes can only bend the flat sheet of metal at discrete bending locations, leaving flat (straight) segments between bends. This fact needs to be considered in shape optimisation algorithms to obtain manufacturable cross-sections.

3.2. Simple manufacturing rules

Simple manufacturing rules have been defined based on basic roll-forming constraints encountered by a European steel storage rack manufacturer. They consist of three main rules:

(1) The minimum internal bending radius r to steel sheet thickness t ratio is equal to 1.0, as shown in Fig. 3.
(2) The minimum length of a single flat segment is equal to 0.394 inch (10 mm), as shown in Fig. 3.
(3) The maximum number of flat segments per cross-section is limited to 20 (i.e. a maximum number of 19 bends per open cross-section).

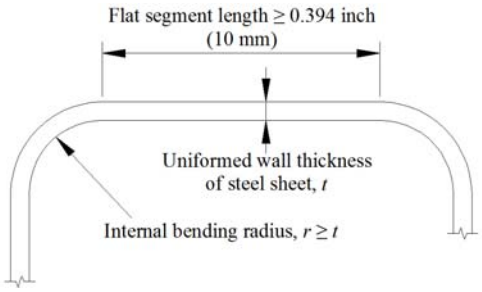

Fig. 3. Manufacturing rules

In the present paper Rule (1) is neglected and only Rules (2) and (3) are considered. A nil internal bending radius (i.e. perfect bends) is assumed to simplify the algorithm. Actual bending radii can be added to the optimised cross-section prior to manufacture.

3.3. Hough transformation

The Hough transformation is used in this paper to detect straight lines, i.e. flat manufacturable segments, in the cross-section. This transformation is commonly used in image processing to detect regular shapes, such as straight lines, circles and ellipses, from the discrete points forming the image (Lee, 2006).

The method consists of defining a "parametric space" in which each straight line in the image is represented by its orientation angle θ, with respect to the Cartesian x-axis, and its normal distance r to the origin, as shown in Fig. 4(a). If θ is restricted to the interval [0˚; 180˚[, each straight line is represented by an unique coordinate (r, θ) in the parametric space. An image point of coordinate (x_i, y_i) in the Cartesian x-y space is transformed into a sinusoidal curve in the parametric r-θ space as

$$r = x_i \cos\theta + y_i \sin\theta \tag{3}$$

Sinusoidal curves having common intersecting points have collinear (aligned) points in the image. This is illustrated in Fig. 4(b) with 4 points aligned on the line of coordinate (r = 0.394 inch (10 mm), θ = 60˚) in the parametric space.

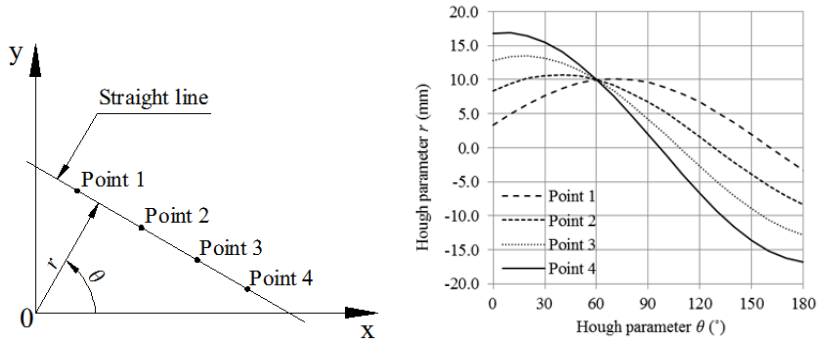

(a) Cartesian coordinate system (b) Hough parameter space

Fig. 4. Hough transformation from Cartesian space to Hough parametric space

For image processing purposes, an array referred to as the accumulator array (or accumulator matrix), is created in the discretised parametric space. The columns of the array corresponds to the increasing values of θ, in $\Delta\theta$ intervals, and the lines to increasing values of r, in Δr intervals. Aligned image points are detected as,

- Step 1: Set $\theta = 0˚$.
- Step 2: For each image point (i) calculate its r value from Eq. (3) for the set value of θ, (ii) calculate the closest discrete r value matching the lines of the accumulator array and (iii) add the point reference number to the corresponding cell in the accumulator array.
- Step 3: Set $\theta = \theta + \Delta\theta$. If $\theta \geq 180˚$ go to Step 4, else go to Step 2.

- Step 4: All points sharing the same cell in the accumulator array are considered aligned.

The choice of the intervals $\Delta\theta$ and Δr influences the ability and accuracy of the Hough transformation to detect straight lines. The smaller $\Delta\theta$, the more refined the search space. A larger value of Δr represents a less stringent alignment tolerance, as illustrated in Fig. 5. Two values of Δr are also shown. A larger Δr_1 results in all the four points in Fig. 5 being aligned by the Hough transformation. A smaller Δr_2 results in only two points being aligned by the Hough transformation.

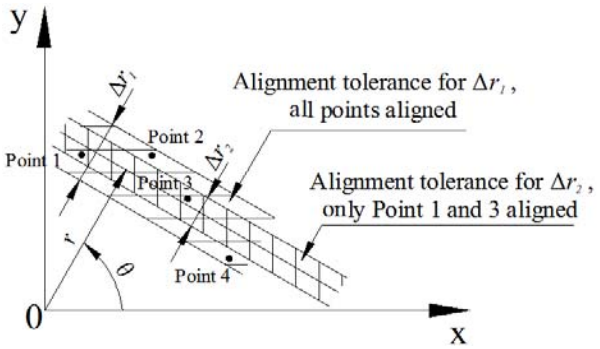

Fig. 5. Alignment tolerance for Hough transformation

3.4. Manufacturing constraints in GA

The manufacturing constraints are introduced into the fitness function (see Eq. (1)) as an equality constraint h_{align}, expressed as

$$h_{align} = \omega \left| \frac{nbAligned}{nbElement} - 1 \right| \tag{4}$$

where ω is a weight associated with the constraint, *nbElement* is the total number of elements of the cross-section and *nbAligned* represents the sum of the N_{max} longest non-concurrent flat segments of the cross-section. N_{max} corresponds to a maximum number of flat segments set by the manufacturer, with N_{max} less than or equal to the maximum possible number of flat segments defined in Rule (3) outlined in Section 3.2. In the algorithm, a flat segment is determined from the Hough transformation as consecutive aligned cross-sectional elements of total length equal to or greater than the minimum manufacturable length as

defined in Rule (2). If the cross-section is made of less than N_{max} flat segments, the constraint is considered satisfied and $h_{align} = 0$.

4. Validation

4.1. Optimisation problem

A similar optimisation problem to the one used in Gilbert et. al. (2012a), for which an analytical solution exists, is considered herein to validate the accuracy of the algorithm to optimise manufacturable cross-sectional shapes. It consists of minimising the cross-sectional area A_s of a thin-walled doubly-symmetric closed cross-section for given second moments of area, I_{xt} and I_{yt}, about the two axes of symmetry. Ragnedda and Serra (2005) indicated that, when $I_{xt} = I_{yt}$, the optimised cross-section is a circle and therefore a regular polygon of n sides if the cross-section is manufactured with n flat segments.

A regular octagon (8 segments) of apothem (at mid-wall thickness) a of 0.790 inch (20 mm) and wall thickness t of 1 mm (0.039 inch) is used herein to verify the algorithm. The cross-sectional area of the octagon A_o is equal to 0.205 inch^2 (132.55 mm^2) and its given second moments of area I_{xt} and I_{yt} are 0.067 inch^4 (28043.3 mm^4). As the problem is doubly-symmetric, only a quarter of the cross-section is considered and the maximum number of flat segments N_{max} is therefore set to 2. The fitness function f derived from Eqs. (1) and (3) is expressed as

$$f = \frac{A_s}{A_o} + \alpha_x \max\left(0, 1 - \frac{I_x}{I_{xt}}\right) + \alpha_y \max\left(0, 1 - \frac{I_y}{I_{yt}}\right) + \alpha_{align}\omega \left| \frac{nbAligned}{nbElement} - 1 \right| \qquad (5)$$

where I_x and I_y are the calculated second moments of area of the cross-section, and α_x, α_y and α_{align} are penalty factors associated with each constraint. In Eq. (1), the constraints on the given second moments of area I_{xt} and I_{yt} are expressed as inequality constraints. This does not penalise the algorithm if $I_x \geq I_{xt}$ or $I_y \geq I_{yt}$ and significantly improves convergence.

The optimum octagon is illustrated in Fig. 6. The circle with the same second moments of area and wall thickness of the octagon is also given in this figure for comparison. The cross-sectional area A_c of the circle is equal to 0.202 inch^2 (130.31 mm^2), i.e. 1.7% less than that of the manufacturable octagon.

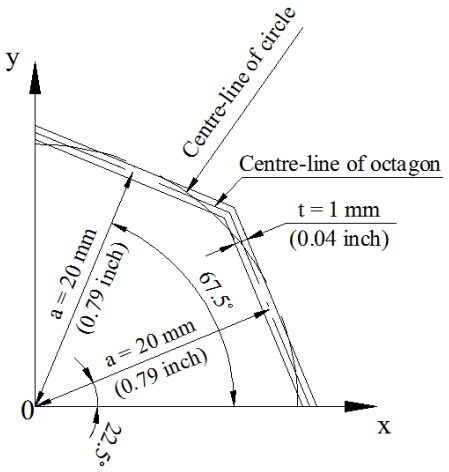

Fig. 6. Optimum octagon, only a quarter section shown

The Augmented Lagrangian fitness function used in the algorithm and derived from Eqs. (2) and (5) is given as

$$Minimise\ f = \frac{A_s}{A_o} + \frac{1}{2}\left\{\gamma_x\left[max(0, 1 - \frac{I_x}{I_{xt}} + \mu_x)\right]^2 + \gamma_y\left[max(0, 1 - \frac{I_y}{I_{yt}} + \mu_y)\right]^2 + \gamma_{align}\left[\omega\left|\frac{nbAligned}{nbElement} - 1\right| + \mu_{align}\right]^2\right\} \quad (6)$$

where γ_x, γ_y and γ_{align} are the Augmented Lagrangian (AL) penalty function coefficients, μ_x, μ_y and μ_{align} are the real parameters associated with each penalty function coefficient. Initial values of $\gamma_x = \gamma_y = 2$ are used herein (Gilbert et. al., 2012a). A lower value of $\gamma_{align} = 0.1$ is used and found to prevent premature convergence of the algorithm. Initial values of $\mu_x = \mu_y = \mu_{align} = 0$ are used, as recommended in Belegundu and Arorat (1984). Additionally, preliminary studies showed that a value of the fixed weight $\omega = 0.5$ with the previously obtained values of γ_x, γ_y and γ_{align} allows the algorithm to align the elements without premature convergence. It may be noted that the use of $\omega = 0.5$ combined with the penalty function coefficient $\gamma_{align} = 0.1$ tends to provide better results than if solely a Lagrangian penalty function coefficient was used (i.e. $\omega = 1.0$).

4.2. Other parameters

An AL penalty increasing constant β of 1.05 and a convergence rate α of 1.5, as advised in Adeli and Cheng (1994) and Gilbert et. al. (2012a), are also used. The design space is set to 1.575 inch × 1.575 inch (40 mm × 40 mm) (Gilbert et. al., 2012a) and the maximum number of generations is set to 150 per run. 10 runs are performed. The number of individuals is set to 700 per generation and the cross-sections are drawn with elements of nominal length of 0.079 inch (2 mm) (see Gilbert et. al. (2012a, b) for more details). The probabilities of cross-over and mutation operations in GA are equal to 80% and 5%, respectively, as used by Gilbert et. al. (2012a).

For the Hough transformation, preliminary parametric studies showed that the values of $\Delta\theta$ equal to 0.5˚ and Δr equal to 0.020 inch (0.5 mm) (see Section 3.3) provide good convergence of the algorithm with a reasonable computational time (about 4 hours per run on a 792 core HPC cluster consisting of a mixture of SGI Altix XE and SGI® Rackable™ C2114-4TY14 servers at Griffith University, Australia).

4.3. Results and discussion

Fig. 7 plots the average fitness function f given in Eq. (5) over 10 runs with penalty factors $\alpha_x = \alpha_y = \alpha_{align} = 10$ and $\omega = 0.5$. The algorithm rapidly converges till the 50th generation and converges to the optimised solution in about 100th generation.

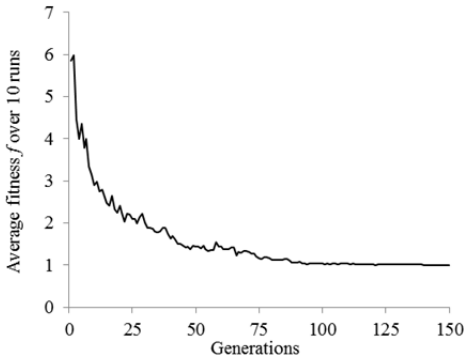

Fig. 7. Average fitness f

Table 1 summarises the average results over 10 runs compared to the known optimum. A negative sign in Table 1 means that the optimised results are less than the optimum. The comparison demonstrates that the algorithm is able to accurately converge to the optimum solution. The average error is -0.4% (CoV = 0.002) for the cross-sectional area and +0.1% (CoV = 0.002) for the second moments of area about the two axes of symmetry. The optimised cross-sections led to the cross-sectional area less (i.e. more optimal) than that of the octagon due to the alignment tolerance in the Hough transformation (see Section 3.3). The algorithm tends to form a cross-sectional shape as closed as a circle, within the alignment tolerance. The larger the alignment tolerance, the closer the cross-section to a circle. The algorithm also aligns the cross-sectional elements to two flat segments for all 10 runs.

Alignment penalty factor	**Cross-sectional area A_s**		**Second moment of area I_x**		**Second moment of area I_y**		***nbAligned/ nbElement***	
	Error (%)	CoV	Error (%)	CoV	Error (%)	CoV	Error (%)	CoV
$\omega = 0.5$	-0.4	0.002	+0.1	0.002	+0.1	0.003	0.0	0.000

Table 1. Average results over 10 runs

Fig. 8 shows the evolution of the cross-sections of the fittest run over six representative generations. Only the mid lines of the cross-section wall thickness are plotted in Fig. 8. The alignment tolerances in the Hough transformation (refer to Section 3.3) for each of the two segments are also shown in the figure. The cross-section is composed of only two flat segments at about generation 50 in Fig. 8(c), i.e. at about one third of the total number of generations. Yet, the segments do not exactly correspond to the optimum octagon at this stage. From the 50th generation onwards, the algorithm refines the search to an optimum octagon.

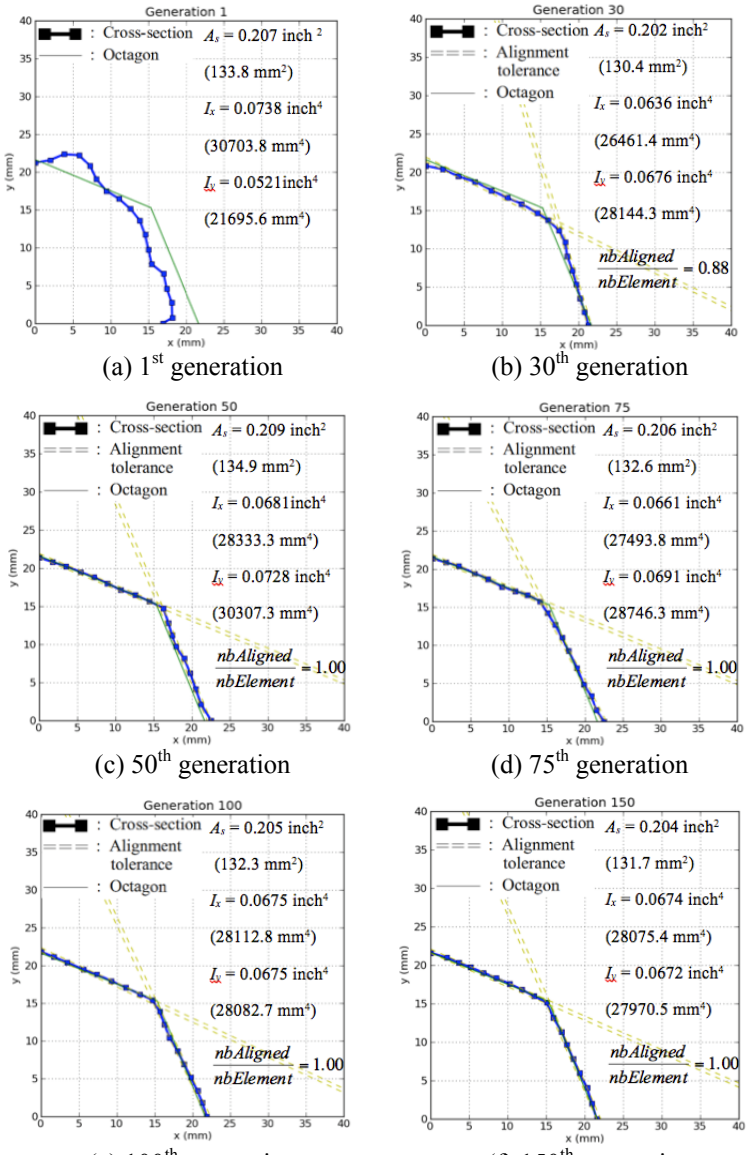

(a) 1st generation (b) 30th generation

(c) 50th generation (d) 75th generation

(e) 100th generation (f) 150th generation

Fig. 8. Cross-sectional evolution for the fittest run over six representative generations from (a) 1st to (f) 150th generation

Fig. 9 plots the optimised cross-sections, with the wall thickness of 0.0394 inch (1 mm) shown, at the 150th generation (final generation) for the two less fit and two fittest cross-sections out of ten runs. It can be seen that the algorithm is able to obtain optimised cross-sections similar to the optimum octagon.

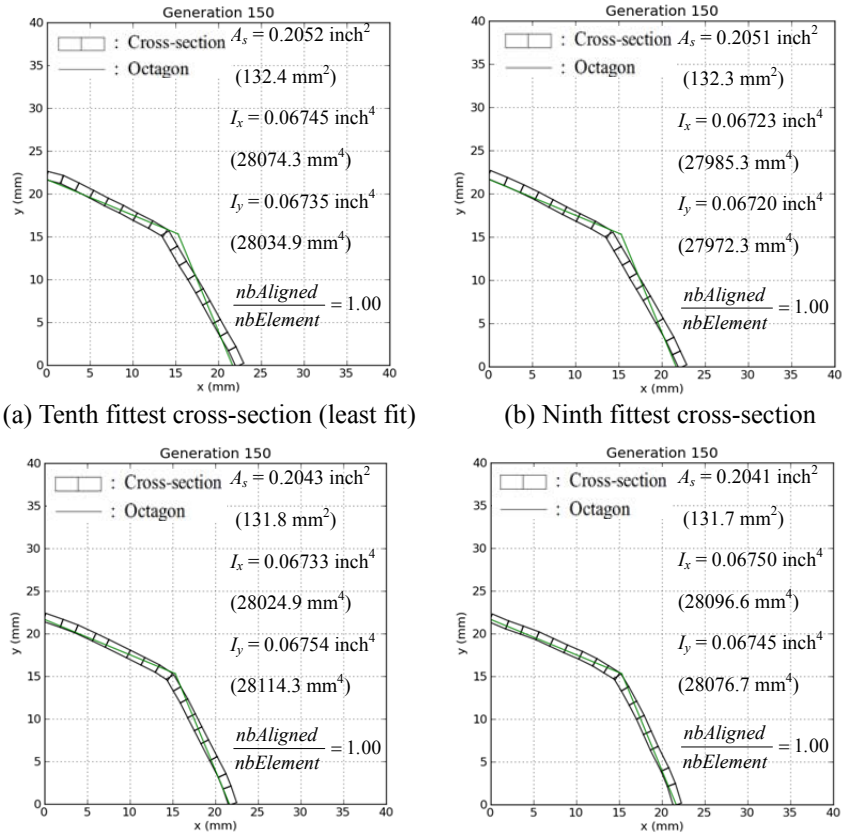

(a) Tenth fittest cross-section (least fit) (b) Ninth fittest cross-section

(c) Second fittest cross-section (d) Fittest cross-section

Fig. 9. Optimised cross-sections at the final generation from the two less fit ((a) and (b)) and the two fittest ((c) and (d)) cross-sections

5. Conclusion

This paper has defined a set of simple manufacturing rules which are incorporated into a previously developed shape optimisation algorithm for CFS profiles. The accuracy of the extended algorithm is verified against an optimisation problem with an existing analytical solution. The algorithm is

proven to be able to accurately converge to known manufacturable cross-sections, with an average error of 0.4% on the cross-sectional area. This algorithm is used in the companion paper (Wang et. al., 2014) to demonstrate an optimised solution for CFS manufacturable columns.

References

Adeli H, Cheng N "Augmented Lagrangian Genetic Algorithm for Structural Optimization", *Journal of Aerospace Engineering*, 7, 104-118, 1994.

Adeli H, Sarma KC, Evolutionary Computing and the Genetic Algorithm, in: Cost Optimization of Structures, John Wiley & Sons, Ltd, 2006, pp. 37-52.

Belegundu AD, Arorat JS "A computational study of transformation methods for optimal design", *AIAA journal*, 22, 535-542, 1984.

Franco JMS, Duarte JP, Batista EdM, Landesmann A "Shape Grammar of steel cold-formed sections based on manufacturing rules", *Thin-Walled Structures*, 79, 218-232, 2014.

Gilbert BP, Teh LH, Guan H "Self-shape optimisation principles: Optimisation of section capacity for thin-walled profiles", *Thin-Walled Structures*, 60, 194-204, 2012a.

Gilbert BP, Savoyat TJM, Teh LH "Self-shape optimisation application: Optimisation of cold-formed steel columns", *Thin-Walled Structures*, 60, 173-184, 2012b.

Griffiths DR, Miles JC "Determining the optimal cross-section of beams", *Advanced Engineering Informatics*, 17, 59-76, 2003.

Hancock GJ, *Design of cold-formed steel structures (to AS/NZ 4600:2007) - 4th Edition*, (Australian Steel Institute), North Sydney, Australia, 2007.

Holland JH, *Adaptation in natural and artificial systems*, (University of Michigan Press), 1975.

Lee J, Kim S-M, Park H-S, Woo B-H "Optimum design of cold-formed steel channel beams using micro Genetic Algorithm", *Engineering Structures*, 27, 17-24, 2005.

Lee K, Application of the Hough transform, University of Massachusetts, Lowell, USA, 2006.

Leng J, Guest JK, Schafer BW "Shape optimization of cold-formed steel columns", *Thin-Walled Structures*, 49, 1492-1503, 2011.

Leng J, Li Z, Guest JK, Schafer BW, "Constrained shape optimization of cold-formed steel columns", *Proceedings of the 21st International Specialty Conference on Cold-Formed Steel Structures*, St. Louis, MO; United States, 59-73, 2012.

Leng J, Li Z, Guest JK, Schafer BW, "Shape optimization of cold-formed steel columns with manufacturing constraints and limited number of rollers",

Proceedings of the Structural Stability Research Council Annual Stability Conference, 313-331, 2013.

Liu H, Igusa T, Schafer B "Knowledge-based global optimization of cold-formed steel columns", *Thin-Walled Structures*, 42, 785-801, 2004.

Lu W, Mäkeläinen P "Fuzzy optimization of cold-formed steel sheeting using genetic algorithms", *Journal of Constructional Steel Research*, 62, 1276-1281, 2006.

Moharrami M, Louhghalam A, Tootkaboni M "Optimal folding of cold formed steel cross sections under compression", *Thin-Walled Structures*, 76, 145-156, 2014.

Ragnedda F, Serra M "On optimum thin-walled closed cross section", *Structural and Multidisciplinary Optimization*, 30, 233-235, 2005.

Schafer BW "Review: the direct strength method of cold-formed steel member design", *Journal of Constructional Steel Research*, 64, 766-778, 2008.

Wang B, Gilbert BP, Molinier AM, Guan H, Teh LH, "Shape optimisation of cold-formed steel profiles with manufacturing constraints: Part II Applications (companion paper)", *Proceedings of the 22nd International Specialty Conference on Cold-Formed Steel Structures*, St. Louis, Missouri, USA, 2014.